Resonant-Inductive Degeneration for a Fourfold Phase-Noise Improvement of a 5.7GHz-Band VCO

Aleksandar Tasić, Wouter A. Serdijn, John R. Long and David L. Harame*

Electronics Research Laboratory/DIMES, Delft University of Technology
Mekelweg 4, 2628 CD Delft, The Netherlands
* IBM Microelectronics, Burlington VT, USA
Phone: +31 (0)15 278 9423; Fax: +31 (0)15 278 5922; E-mail: a.tasic@ewi.tudelft.nl

Abstract. Resonant-inductive degeneration of tail-current noise in a VCO is presented in this paper. Two test oscillators are described: one designed with, and the other without resonant degeneration. By forming a resonance at twice the oscillation frequency in the emitter of the bias current source, phase noise is improved by 6dB. Phase noise of –112dBc/Hz at 1MHz offset from a 5.7GHz–band carrier and a 5.45-6.05GHz frequency tuning range are realized using oscillator with resonant-inductive degeneration, while drawing 4.8mA from a 2.2V supply.

I. INTRODUCTION

Low-noise voltage-controlled oscillators (VCOs) are required for local signal generation in a variety of portable wireless applications. The contribution of the bias tail-current source noise of a bipolar VCO to the phase noise is larger than all other noise contributions put together (i.e., LC-tank noise and transconductor noise), in a well-designed circuit [1]. In particular, tail-current noise at twice the oscillation frequency is converted to the fundamental by limiting in the gain stage of the oscillator, and cannot be attenuated by the resonator.

Therefore, the noise-optimization procedure proposed in this paper is focused on reducing noise generated by the tail current source at twice the oscillation frequency (i.e., $2f_0$). Resonating a degeneration inductor with the base-emitter capacitance of the bias transistor at $2f_0$ effectively reduces the output current noise density that is converted by hard switching into phase noise of the oscillator. We call this "resonant-inductive degeneration" (RID). It is suitable for low-voltage applications as it requires no d.c. voltage headroom. The RID inductor in the low-nH range occupies a relatively small chip area when fabricated using the multiple layers of metal available in modern silicon VLSI technologies.

The transformations of the base-resistance noise, base-current and collector-current shot noise sources of the resonant-inductive degenerated tail-current source transistor are described in Section II of this paper. Section III outlines oscillator circuit parameters.

Measured performance of oscillators designed with and without resonant-inductive degeneration is detailed in Section IV of this paper. Both oscillators operate from a 2.2V supply with a frequency tuning range of 600MHz, (5.45-6.05GHz). At 1MHz offset from a 5.7GHz-band carrier (i.e., the upper 802.11a/HIPERLAN band), the oscillator with RID achieves a phase noise of -112dBc/Hz. This is a 6dB improvement in phase noise compared to the control VCO, which does not use RID in the bias source. RID reduces phase noise sufficiently to satisfy the phase-noise requirements of either 802.11a or HiperLAN [2], while dissipating only 10.6mW.

II. RESONANT-INDUCTIVE DEGENERATION

The bipolar VCO shown in Fig. 1 is used to implement the 802.11a/HIPERLAN oscillator. L is the tank inductance, C_V the tank varactor capacitance, C_A and C_B are the quasi-tapping feedback capacitances, V_{CC} is the supply voltage, V_B the base bias voltage, and I_{TAIL} the bias current.

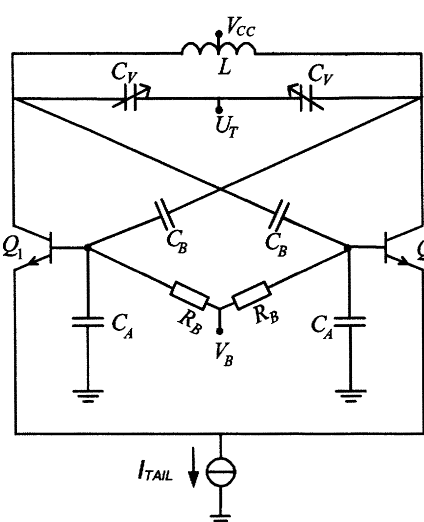

Figure 1. LC-oscillator.

One realization of the bias tail-current source (TCS) is shown in Fig. 2, together with its noise sources ($\overline{V}_{B,CS}$ is the base-resistance thermal noise, $\overline{I}_{B,CS}$ the base-current shot noise and $\overline{I}_{C,CS}$ the collector-current shot noise). The output current noise density of the tail-current source can be calculated after transforming noise sources to the output,

$$\overline{I}_{CS}^{2} = 4kT\frac{g_{m,CS}}{2}\left[1+2r_{B,CS}g_{m,CS}\right] \qquad (1)$$

$g_{m,CS}$ is the transconductance and $r_{B,CS}$ the base resistance of the TCS transistor Q_{CS}, T is absolute temperature, and k is Boltzmann's constant.

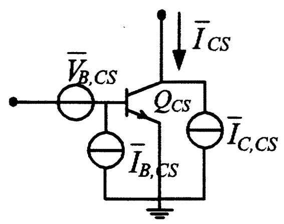

Figure 2. Tail-current source transistor and its noise sources.

Simulations show that the contribution of noise from the bias tail-current source around even multiples of the oscillation frequency to the phase noise of the oscillator is larger than all other oscillator noise contributions combined. In particular, the tail-current noise around twice the oscillation frequency ($2f_0$) has the largest contribution to the phase noise of the oscillator after being converted to the resonating LC-tank by the switching of transconductor Q_1-Q_2.

Resonant-inductive degeneration [3] is a design procedure proposed to minimize the noise contribution of the oscillator's tail-current source. It relies on forming a resonance between the inductor (L_{RID}) in the emitter of the tail-current source transistor Q_{CS} and its base-emitter capacitance $C_{\Pi CS}$ at $2f_0$ (see Fig. 3). This results in reduction of contributions of base-resistance thermal noise and collector-current shot noise of bias TCS to oscillator's phase noise. The noise reduction is due to high impedance in the emitter of the RID TCS transistor and its reduced gain at resonance.

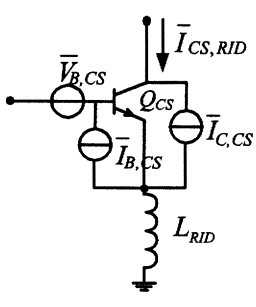

Figure 3. Resonant-inductive degenerated tail-current source transistor and its noise sources.

We will determine the performance of resonant-inductive degeneration by calculating transfer functions from the base-resistance noise, base-current shot noise and collector-current shot noise sources to the output of the current source shown in Fig. 3.

A. Base-Resistance Noise Transformation

The input impedance of an inductively degenerated transistor (see Fig. 3) is given by [4]:

$$Z_{IN}(f) = 2\pi f_{T,CS}L_{RID} + j\left[2\pi fL_{RID} - \frac{f_{T,CS}}{f}\frac{1}{g_{m,CS}}\right] \qquad (2)$$

For the RID at $2f_0$, the imaginary part of Eq. 2 is set to zero. Then

$$R_{IN}g_{m,CS} = \left(\frac{f_{T,CS}}{2f_0}\right)^2 \qquad (3)$$

where $f_{T,CS}$ is the transit frequency of Q_{CS} and R_{IN}=$2\pi f_T L_{RID}$ is equal to the real part of the impedance at the base of Q_{CS} as seen from Eq. 3.

The equivalent transconductance of the RID tail current-source transistor at $2f_0$ now equals [4]:

$$g_{EQ,CS} \cong -\frac{1}{R_{IN,CS}}\frac{f_{T,CS}}{2f_0} \qquad (4)$$

and the contribution of the noise from the base resistance to the output current noise density of the degenerated tail-current source becomes:

$$g_{EQ,CS}^{2}\overline{V}_{B,CS}^{2} = g_{m,CS}^{2}\left(\frac{2f_0}{f_{T,CS}}\right)^2 4KTr_{B,CS} \qquad (5)$$

This suggests that a reduction of the TCS base-resistance thermal noise is possible for $2f_0/f_{T,CS}$<1.

B. Base- and Collector-Current Shot Noise Transformations

With the aid of Fig. 4, we will first determine the transfer function for collector-current shot noise $I_{C,IN}$ to the output of the current source I_{OUT} by applying superposition (i.e., $I_{B,IN}$=0).

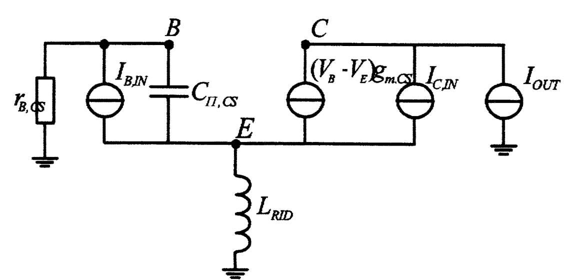

Figure 4. RID tail-current source (a detailed schematic).

First analyzing the BE branch in Fig. 4, the relationship between the base-emitter voltage (V_{BE}) and the current $I_{C,IN}$ can be determined. At the resonant frequency ($2f_0$) between L_{RID} and $C_{\Pi,CS}$, this becomes:

$$I_{C,IN} = -V_{BE}\left[g_{m,CS} + \frac{C_{\Pi,CS} r_{B,CS}}{L_{RID}} \right]. \quad (6)$$

Referring to node C, the transfer function from the collector current noise source to the output of the TCS at $2f_0$ is:

$$\frac{I_{OUT}}{I_{C,IN}}(2f_0) = 1 - 1/[1 + r_{B,CS} g_{m,CS} (\frac{2f_0}{f_{T,CS}})^2] \cong 0. \quad (7)$$

As $r_{B,CS}g_{m,CS}$ is a small constant, and $2f_0/f_{T,CS}<<1$, the collector-current shot noise is suppressed from the output current noise of the TCS.

In a similar manner, the transformation of the base-current shot noise to the output of the TCS is calculated from Fig. 4 ($I_{C,IN}$=0). The resulting transfer function at $2f_0$ becomes:

$$\frac{I_{OUT}}{I_{B,IN}}(2f_0) = 1/[1 + r_{B,CS} g_{m,CS} (\frac{2f_0}{f_{T,CS}})^2] \cong 1 \quad (8)$$

implying that the base-current shot noise is transferred completely to the output of the tail-current source.

C. Total Output Noise of RID TCS

Combining Eqs. 5 and 8 (i.e., the base resistance thermal and the base-current shot noise contributions), the total output current noise density of the resonant-inductive degenerated tail-current source becomes:

$$\overline{I}^2_{CS,RID} = 4kT\frac{g_{m,cs}}{2}\left[\frac{1}{\beta_F} + 2r_{B,CS}g_{m,cs}\left(\frac{2f_0}{f_{T,CS}}\right)^2\right]. \quad (9)$$

A comparison of Eq. 1 (noise of tail-current source without degeneration) and Eq. 9 suggests that by applying resonant-inductive degeneration, the contribution of the tail-current noise from $2f_0$ is reduced by more than $(f_{T,CS}/2f_0)^2$ (e.g., a factor of 100 for $f_{T,CS}/2f_0 = 10$).

Note that minimizing or eliminating the noise contribution of the TCS improves phase noise performance of the VCO, or it permits operation at a lower bias current for the oscillator under consideration.

III. OSCILLATOR CIRCUIT PARAMETERS

The test oscillator bias and circuit parameters are optimized for the lowest phase noise.

For a supply voltage of 2.2V, a transconductor base bias voltage V_B of 1.85V is chosen. It allows for both the largest voltage swing of the output signal and the most efficient use of the voltage headroom available. Maximum voltage swing is estimated from the saturation condition of the transconductor transistors, in order to avoid noise injection of the forward-biased base-collector junctions. For a tapped capacitor ratio n=1+(C_A+C_Π)/C_B of 1.6, a maximum voltage swing across the bases of the transconductor $v_{S,B,MAX}$ of 0.68V is obtained, corresponding to a small-signal loop gain of around 10.

For effective suppression of the tail-current source noise at twice the oscillation frequency (i.e., between 11GHz and 12GHz), a symmetric resonant-degenerative inductor of 2.6nH (2xL_{RID}) was integrated in a 1.25um thick metal. It has 7 turns, outer diameter of 106um, metal width of 5um, and metal spacing of 1.5um. A small resistor (30Ω) was added in series with the degenerative inductor. Although this has minor effect on high-frequency tail-current noise, it aids suppression of low-frequency TCS noise and improves temperature stability of the oscillator. It should be noted that a multi-layer inductor would also be suitable for L_{RID} as it requires even less chip area, as long as its self-resonant frequency is sufficiently greater than $2f_0$.

As a compromise between low phase noise, low power consumption and frequency tuning range (aiming for the upper 802.11a/HIPERLAN band), the other oscillator parameters have been determined. The 1.2nH LC-tank inductor was designed using 4um thick aluminum top metal in the 120GHz SiGe technology [5]. This differentially shielded symmetric 2-turn inductor uses a ladder substrate shield, has an outer dimension of 190um, metal width of 10um, and metal spacing of 5um. Two n-type MOS varactors with 40 gates are used to tune the LC-tank. Metal-insulator-metal capacitors C_A and C_B are 100fF and 250fF, respectively.

Two common-collector output buffers interface the oscillator and a 50Ω measurement set-up, each consuming 1.1mA of current.

IV. MEASUREMENT RESULTS

The chip photomicrograph of the voltage-controlled oscillator with resonant-inductive degeneration is shown in Fig. 5 (together with buffer circuits).

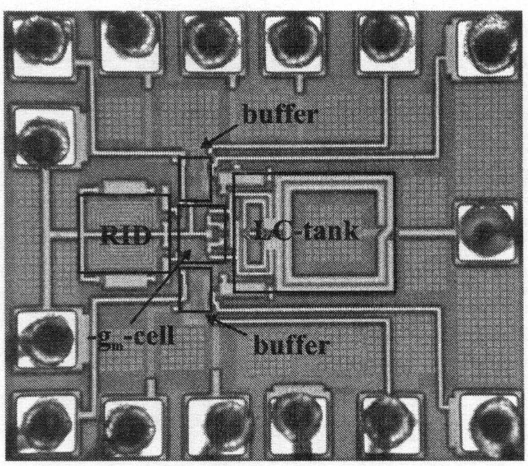

Figure 5. Photomicrograph of the VCO with RID.

Oscillator and buffers occupy an area of 215x490um^2 (0.1mm^2), excluding bondpads. For validation of the resonant-inductive degeneration method, another (identical) voltage-controlled oscillator was designed without resonant-inductive degeneration (i.e., L_{RID} is grounded on both sides), as shown in Fig. 6. The 2 oscillator designs have maximum voltage swing and lowest phase noise for the same power consumption, as they have identical LC-tanks, transconductors and bias tail-current source transistors.

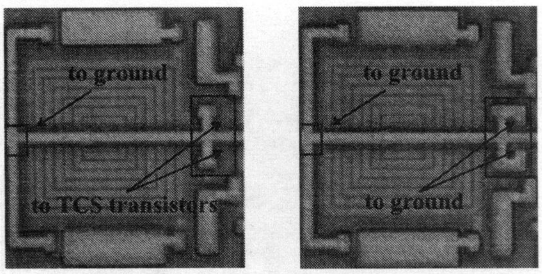

Figure 6. (left) VCO with RID, (right) VCO without RID.

After wirebonding into 32-lead quad packages, the oscillator designs were connected to a printed-circuit board with bias and supply line filtering for testing [6].

A frequency tuning range of 600MHz (5.45GHz-6.05GHz) was measured for a 0.9V tuning voltage range (i.e., between 1.3V and 2.2V) as seen in Fig. 7. The error on the prediction of the oscillation frequency is below 1%. This frequency tuning range covers the upper band of 802.11a and HIPERLAN standards, and with additional MOS capacitors in parallel with the LC-tank the operating frequency could be trimmed to cover the complete 5GHz band. Combined with an injection-lock oscillator [7], this design allows for a multi-standard operation (i.e., 802.11a/HIPERLAN and HIPERLINK modes) as it would be able to cover the 17.1-17.3GHz HIPERLINK band with a large margin.

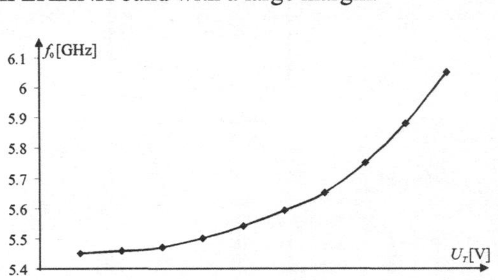

Figure 7. VCO frequency tuning characteristic.

Phase noise properties of the oscillators with and without RID are compared in Fig. 8. For a –12.3dBm output power from a single buffer (i.e., equal RF power levels of both oscillator outputs), the oscillator with the resonant-inductive degenerated tail-current source has 6dB better phase noise at 1MHz offset from the carrier in the 5.7GHz band, compared to the oscillator implemented without RID.

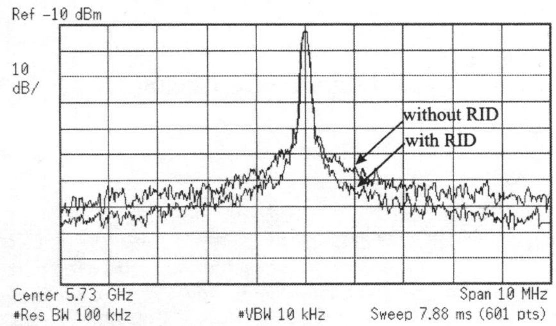

Figure 8. Oscillators' outputs in a 5.7GHz band.

At 1MHz offset in the upper 5.7GHz 802.11a/HIPERLAN band, the oscillator with the resonant-inductive degenerated tail-current source achieves a phase noise of -112dBc/Hz for a current consumption of 4.8mA (see Fig. 8). The power-consumption figure of merit is 177.

V. CONCLUSIONS

Resonant-inductive degeneration in the emitter of the bias tail-current source transistor improves the phase noise of a 5.7GHz VCO by 6dB, resulting in -112dBc/Hz phase noise at 1MHz offset with a power consumption of 10.6mW.

Resonant-inductive degeneration is suitable for low-voltage RF applications, as it requires no d.c. voltage headroom, and a low-nH inductor that can be cost-effectively implemented in any modern multi-layer metal silicon technology.

VI. REFERENCES

[1] E. Hegazi et al., "Filtering Technique to Lower VCO Phase Noise", *Proc. ISSCC,* pp. 364-365, Feb. 2001.

[2] ETSI TC-RES, "Radio Equipment and Systems (RES); High Performance Radio Local Area Network (HIPERLAN); Functional Specification," ETSI, 1996.

[3] A. Tasić, W. A. Serdijn and J. R. Long, "Low-Noise Biasing of VCOs by Means of Resonant-Inductive Degeneration", *Proc. ISCAS,* pp 673-676, May 2003.

[4] S. P. Voinigescu et al., "A Scalable HF Noise Model for Bipolar Transistors with Application to Transistor Sizing for LNA Design", *Journal of SSC*, vol. 32, no. 9, pp. 1430-1439, Sep. 1997.

[5] A. Joseph et al., "A 0.18um 120/100GHz (f_T/f_{MAX}) HBT and ASIC-compatible CMOS using copper interconnect", *Proc. BCTM*, pp. 143-146, Oct. 2001.

[6] A. Tasic, S-T. Lim, W. A. Serdijn and J. R. Long, "A Multi-Standard Adaptive Image-Reject Downconverter", *Proc. RFIC*, pp. 581-583, June 2005.

[7] S. Y. Yue et al. "A 17.1-17.3GHz IR Downconverter with Phase-Tunable LO using 3x Subharmonic IL", *Journal of SSC*, vol. 39, no. 12. pp. 2321-2332, Dec. 2004.